

A theoretical and experimental investigation of material removal characteristics and surface generation in bonnet polishing

Abstract

This paper presents a theoretical and experimental investigation which attempts to provide a better scientific understanding of the material removal characteristics and surface generation in bonnet polishing. The experimental results reveal that the material removal is shared by the polishing pad and the abrasives trapped in the pad-workpiece interface, and the abrasive wear is dominated significantly by plastic removal mode of abrasive particles, while the material removal caused by the polishing pad should be mitigated in order to obtain super mirror finished surfaces. The surface generation is found to be a linearly cumulative effect of dwell time together with the constant material removal rate under the identical polishing condition. Hence, a multi-scale material removal model and a surface generation model have been built based on the contact mechanics, kinematics theory, abrasive wear mechanism, as well as the relative and cumulative removal process of surface generation in bonnet polishing. The models are verified through a series of spot and pattern polishing experiments. Based on the results of spot polishing experiments, the multi-scale material removal model is found to predict well for the material removal characteristics under various polishing conditions. The simulated patterns by the surface generation model are found to agree well with the measured patterns in the pattern polishing experiments which substantiate that the relative and cumulative removal process is a key surface generation mechanism in bonnet polishing.

Keywords: Ultra-precision Machining, Bonnet Polishing, Surface Generation, Modelling, Contact Mechanic, Multi-scale Materials Removal

1. Introduction

Bonnet polishing is a computer controlled sub-aperture polishing process that actively controls the position and orientation of a spinning, inflated, membrane tool (the 'bonnet') as it sweeps through the polished surfaces [1] (see Fig. 1). It is essential for achieving the ever increasing tolerances and demands for high-precision applications such as optical [2], biomedical [3], and automotive components [4]. This is particularly true for machining difficult-to-machine materials which are not amenable to using other ultra-precision machining technologies such as single-point diamond turning and ultra-precision raster milling. Polishing of such materials with sub-micrometre form accuracy and surface finish in the nanometric range is complex and multi-scale in nature. As a result, knowledge of the removal mechanisms and factors affecting material removal characteristics and surface generation are vital to determine the surface quality and form control in the polishing process.

During the past few decades, much research has been performed on the study of the development and application of *precess* polishing process [5, 6], edge control [7], tool path and dwell time

optimization [8, 9], polishing mechanics [10, 11], as well as methods include finite element methods (FEM) [12], molecular dynamics (MD) approach [13], quasic-static model [14], fluid dynamic when analyzing the slurries and probability statistics [15, 16]. Most of the previous research has focused on the reduction of surface roughness and figuring of aspheric and freeform surfaces [17], and some preliminary work has also been done for structured surface generation by bonnet polishing [18]. Although polishing processes have been investigated [19], studies on the polishing mechanisms, especially on the establishment of deterministic models with consideration of all these operational parameters, are still far from complete. This is particularly true for ultra-precision, multi-axis, freeform polishing, which is a kind of non-conventional polishing method that has been used for machining ultra-precision freeform components that require precise control and accuracy across the polishing surface to maintain the form and achieve nanometric surface finish, which improve the functionality of the components.

As a result, an experimental and theoretical investigation of materials removal characteristics and surface generation in bonnet polishing is undertaken which is basically divided into two parts i.e. Part A and Part B. In Part A, a series of polishing experiments were conducted to better understand the material removal and surface generation mechanisms in bonnet polishing. In Part B, a multi-scale material removal model and a surface generation model are built based on contact mechanics, kinematics theory and abrasive wear mechanism. A series of experiments have been conducted for validating the surface topography simulation model. Results and analysis reveal some insights into the polishing process.

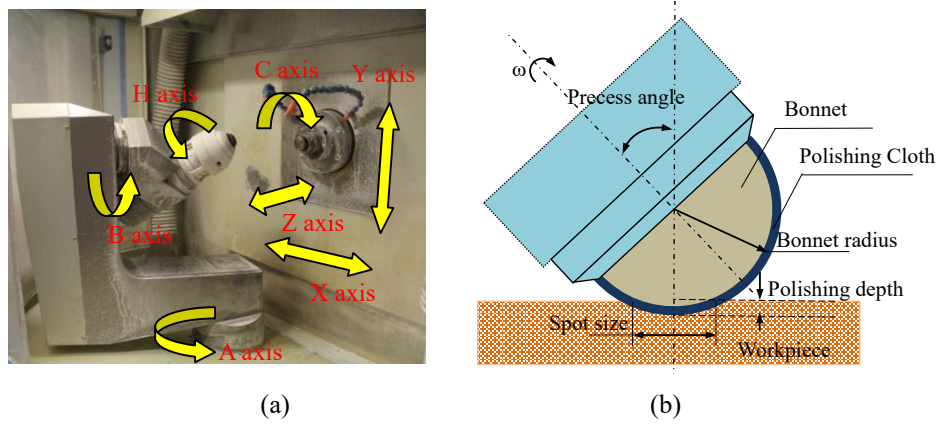


Fig.1 (a) Configure and (b) schematic illustration of bonnet polishing

2. Part A: Experimental Investigation

2.1 Experimental Design

Bonnet polishing is a kind of computer controlled ultra-precision polishing (CCUP) technology. Within the field of CCUP, the material removal characteristics represent the distribution of the material removal rate across the size of the polishing tool. The material removal characteristics are referred to be the tool influence function (TIF) and they are assessed in terms of width, maximum depth and

volumetric material removal rate [20]. Bonnet polishing involves forcing a spinning, inflated bonnet, covered with the polishing pad, against the polished surfaces flooded with a liquid slurry of abrasive particles. The slurry is dragged by the porous polishing pad into the interface between the pad and workpiece. The material removal in bonnet polishing is accomplished by the interactions between the polishing pad, workpiece and abrasive particles. The mechanism of material removal is a complex process, which is affected by various parameters such as tool radius, *precess* angle, polishing depth, head speed, tool pressure, polishing time, polishing cloth, slurry concentration, particle size and material properties of particle and workpiece, etc. To better understand the pad-abrasive-workpiece contact mechanics and polishing mechanisms in bonnet polishing, experiments were conducted to help to explain some common experience as follows: Experiment A1 aims to investigate the interactions among the polishing pad, workpiece and abrasive particles, three samples made of nickel copper (NiCu) were prepared by the Moore Nanotech 350FG using single point diamond tooling and then polished on a Zeeko IRP 200 ultra-precision freeform polishing machine (see Fig.2(a)). Sample A1.1 was polished without water and abrasive particles, sample A1.2 was polished using pure water without abrasive particles and sample A1.3 was polished using a slurry comprising 2.066 vol. % of Al_2O_3 abrasives with an average size of $3.22\text{ }\mu\text{m}$. All these samples were polished under the identical polishing parameters as shown in Table 1 and they are measured by a Zygo Nexview 3D Optical Surface Profiler (see Fig.2(b)) and HITACHI TM3000 Tabletop Scanning Electron Microscope (see Fig.2(c)). With the consideration of the importance of dwell time map for the surface generation by bonnet polishing, the effect of polishing time on surface generation for various materials were studied in experiment A2. Three samples made of different materials of steel, optical glass (BK7) and Nicu were polished using a slurry comprising 2.066 vol. % of Al_2O_3 abrasives with an average size of $13.12\text{ }\mu\text{m}$. All experiments were conducted on a Zeeko IRP 200 ultra-precision freeform polishing machine using the different polishing time of 60s, 120s and 180s and the other parameters can be seen in Table 1.

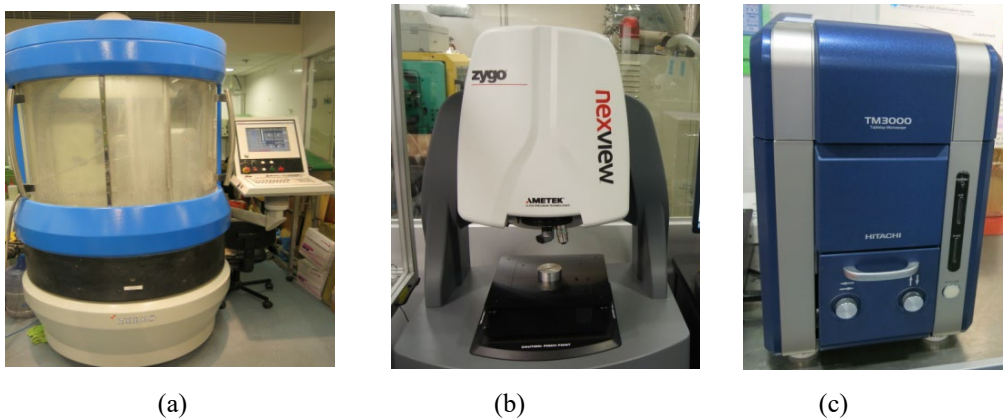


Fig.2 (a) Zeeko IRP200 Ultra-precision freeform polishing machine, (b) Zygo Nexview 3D Optical Surface Profiler and (c) HITACHI TM3000 Tabletop Scanning Electron Microscope

Table 1 Polishing parameters used in the experimental studies

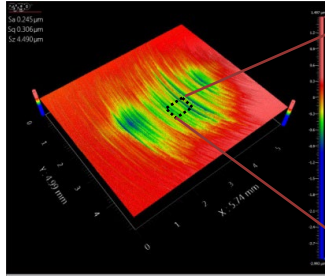
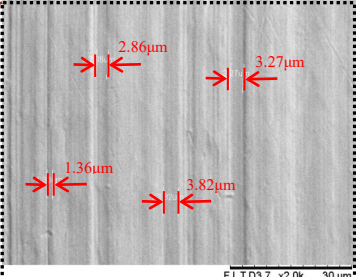
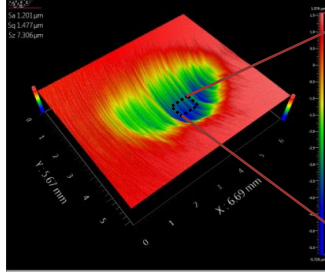
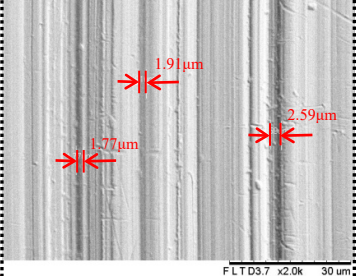
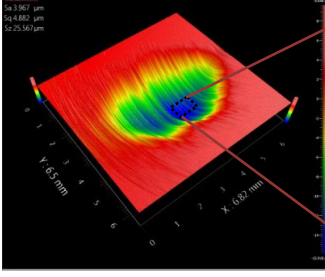
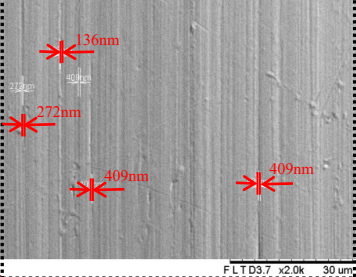
Polishing pad	LP-66 (Cerium oxide D'27)
<i>Precess</i> angle	15°
Tool size	20 mm radius bonnet
Tool pressure	1.2 bar
Polishing depth	0.2 mm
Head speed	1200 rpm
Polishing time	60s

2.2 Results and Discussion in Part A

2.2.1 Pad-abrasive-workpiece Interactions

In experiment A1, Table 2 shows that sample A1.3 has the highest material removal rate while the amount of material removal of sample A1.2 is smaller than that of sample A1.3, and sample A1.1 has the lowest material removal. It is also found that the polishing pad not only contributes to the material removal but also generates micro-scale scratches on the polished surface as shown in the scanning electronic microscopy (SEM) photographs in Table 2. The outcomes of these experiments can be summarized as follows: (i) The interaction between the pad and the polished surface decreases the material removal rate for the dry bonnet polishing process; (ii) The functions of the abrasive slurry in bonnet polishing including transport of abrasive to a loose abrasive process, flushing or the transport of the debris away from the abrasive process, culling in the contact area, mechanical lubrication of the abrasive contacts, etc. (iii) The material removal in bonnet polishing is shared by the polishing pad and the abrasives trapped in the pad-workpiece interface, and the amount of material removal by the polishing pad is much smaller than that by the abrasive particles. More importantly, the material removal produced by the polishing pad is mainly caused by the abrasion associated with plastic deformation of the polishing pad and could produce the scratches and hence damage the surfaces being polished. To obtain super mirror finished surfaces without pad scratches, abrasive wear occurred in bonnet polishing which is dominated by plastic removal mode of abrasive particles, while the material removal caused by the polishing pad should be mitigated through flatting the asperities [21-23], controlling reasonably the polishing depth and/or adopting appropriately the polishing pad owned low pad hardness.

Table 2 Experimental results for studying interactions between the pad, workpiece and particles

Sample No.	Zygo photographs	SEM photographs (Center area)
A1.1 (No water and no abrasive particles)		
A1.2 (with water but no abrasive particles)		
A1.3 (with water and abrasive particles)		

2.2.2 Effect of Polishing Time

Since the surface generation by bonnet polishing is dominated by the influence function of the polishing tool instead of the geometry of the cutting tool itself, the surface generation mechanism of bonnet polishing is quite different from that of other ultra-precision machining processes such as single point diamond turning and raster milling [18]. The tool influence function (TIF) affected by various factors is commonly regarded as a tool that is used in calibration, prediction or form correction in the polishing process. With the data of the tool influence function, the polishing tool can be commanded where it should stay longer or shorter for removing more or less materials from the surface, respectively. In experiment A2, Fig.3 shows that the removal volume increases linearly with increasing polishing time for all cases and this infers that the material removal rate is constant when using only polishing time as a variable parameter while keeping other parameters constant. This infers that bonnet polishing is a relative and cumulative polishing process for various materials and the surface generation of bonnet polishing is a linearly cumulative effect of dwell time together with the constant material removal rate for identical polishing condition.

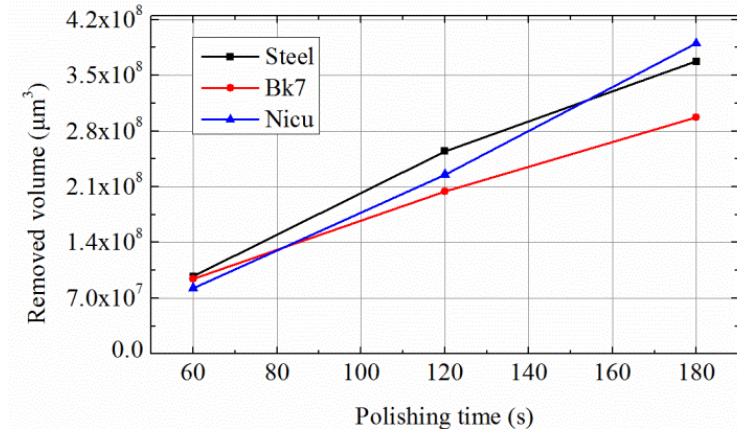


Fig. 3 The effect of polishing time on the surface generation

3. Part B: Theoretical Investigation of Materials Characteristics and Surface Generation

3.1 Theoretical Modelling and Simulation

It is well known that the surface generation of the polishing process can be regarded as the convolution of the influence function and the dwell time map along the pre-specific tool path. Hence the determination of the material removal characteristics and an optimized tool path generator are of paramount importance for modelling and simulation of the surface generation in bonnet polishing. In Part B, a multi-scale material removal model is developed by the study of the contact mechanics, kinematics theory and abrasive wear mechanism. Then the polishing tool path is planned based on the desired surface integrity of the optical surface to be generated using the predicted data of the material removal characteristics. Finally, the surface generation is simulated based on the developed multi-scale material removal model and polishing tool path planning.

3.1.1 Multi-scale material removal model

Based on the experimental results of section 2.2.1, the material removal caused by the polishing pad is much less than that caused by the abrasive particles. Hence, an assumption can be made that material removal occurs primarily as a result of abrasive wear of the surface by the abrasive particles in the slurry. From the view of the mechanical behavior, the basic model of the material removal characteristics of bonnet polishing process can be described by Eq. (1) as shown in Fig. 4.

$$MRR(x, y, t) = N(k_{ac}, V_c, t, R_p, R_a, \sigma_z) \cdot E(\eta, P(x, y, R_b, d, \omega, Y, \nu, \phi, \eta_1, \eta_2), V(x, y, S, \phi, R_b, d), H_w, \beta) \quad (1)$$

where $MRR(x, y, t)$ is material removal amount at position (x, y) during the polishing time t . The term $N(k_{ac}, V_c, t, R_p, R_a, \sigma_z)$ is the spatial distribution of active abrasive particles participated in the material removal which represents the effect of the volume fraction V_c , the polishing time t , the radius of the abrasive particle R_p , the pad asperity radius R_a , the standard deviation of asperity heights σ_z , and the coefficient related to the particle size distribution and the hydrodynamics condition k_{ac} . The term $E(\eta, P(x, y, R_b, d, \omega, Y, \nu, \phi, \eta_1, \eta_2), V(x, y, S, \phi, R_b, d), H_w, \beta)$ is the volume removed by a single particle that describes the effect of the pressure distribution

$P(x, y, R_b, d, \omega, Y, \nu, \varphi, \eta_1, \eta_2)$, the velocity distribution $V(x, y, S, \varphi, R_b, d)$, the hardness of polished workpiece H_w , the semiangle of a cone particle β , and a volume fraction of a wear groove removed as a wear debris η .

The slurry particles involved in material removal are those that are embed in the surface of the compliant polishing pad and they are dragged across the polished surface by the relative velocity between two surfaces, and the active number of these particles is generally related to the distribution of particle size, the hydrodynamics condition between the polishing pad and the workpiece, as well as the surface topography of the polishing pad and the target surface. To simplify the theoretical modelling, the pad-particle-workpiece contact is assumed to be solid-solid contact neglecting the effect of the fluid flow, and the particle size is assumed to be constant which is the same as the average size of the particle distribution. In the present study, statistical theories were used to model the surface topography of polishing pad assessed by the pad asperity radius R_a and the standard deviation of asperity heights σ_z [24, 25]. For relatively soft pad and low abrasive concentration, the active number of abrasive particles tends to be proportional to the real contact area and the slurry concentration [26-28]. As a result, the active number of abrasive particles can be expressed by Eq. (2) as follows:

$$N(k_{ac}, V_c, t, R_p, R_a, \sigma_z) = K_{ac} \frac{V_c t}{R_p^2} \left(\frac{R_a}{\sigma_z} \right)^{1/2} \quad (2)$$

The effective contact area between the polishing pad and the entrained particle is approximately equal to πR_p^2 [29], and hence the force applied on an abrasive, W_p , can be expressed by Eq. (3)

$$W_p = \pi R_p^2 P(x, y, R_b, d, \omega, Y, \nu, \varphi, \eta_1, \eta_2) \quad (3)$$

In the bonnet polishing process, since the abrasive particles are sufficiently small and numerous in the contact region, the load carried by each tends to be below the critical value needed to cause cracking. Below this critical value, a hard abrasive particle would cause plastic deformation only, and the wear is undertaken by plastic processes without brittle fracture. Abrasive particles may roll and/or slide over the surface which involve in three distinct modes of plastic deformation including cutting, ploughing and wedge formation [29, 30]. The transition from one mode to another and the relative efficiency of each mode may depend on the attack angle of particle, the normal load, the hardness of the material, and the state of lubrication [31]. In the polishing process, lubrication of the slurry can lead to more particles cutting and reduce the couple necessary for particle rotation by lowering the friction between the particles and the surface [32]. In this study, an abrasive particle, assumed to be a cone of semiangle β , is dragged across the surface in plastic contact which flows under an indentation pressure H_w . Since the depth of indentation, δ_p , is much smaller than the radius of the abrasive, the volume of wear debris produced by the cone particle per unit time can be expressed by Eq. (4) as follows:

$$\begin{aligned} E(\eta, P(x, y, R_b, d, \omega, Y, \nu, \varphi, \eta_1, \eta_2), V(x, y, S, \varphi, R_b, d), H_w, \beta) &= \eta \delta_p^2 \tan \beta V(x, y, S, \varphi, R_b, d) \\ &= \frac{2\eta W_p V(x, y, S, \varphi, R_b, d)}{\pi H_w \tan \beta} = \frac{2\eta R_p^2 P(x, y, R_b, d, \omega, Y, \nu, \varphi, \eta_1, \eta_2) V(x, y, S, \varphi, R_b, d)}{H_w \tan \beta} \end{aligned} \quad (4)$$

According to the kinematics theory, the relative velocity between the polishing pad and the target surface in the polishing area can be expressed as

$$V(x, y, S, \varphi, R_b, d) = \frac{\pi S}{30} \sqrt{(y \cot \varphi - (R_b - d))^2 (\sin \varphi)^2 + x^2 (\cos \varphi)^2} \quad (5)$$

where $x^2 + y^2 \leq (R_b)^2 - (R_b - d)^2$; S is angular velocity in rpm; φ is the inclination angle; d is the polishing depth in mm; R_b is the radius of the bonnet in mm.

The pressure distribution between the polishing pad and the target surface is very complex and still not well understood as resulting from multiple influence factors including the elastic response of the polishing pad, the hydrodynamic forces due to fluid flow at the interface and the viscoelastic relaxation of the polishing bonnet, etc. In this study, the viscoelastic properties of the polyurethane pad is considered, the polishing bonnet in contact with the flat workpiece surface was assumed to be a viscous sphere on a hard plane regardless of the contribution of slurry hydrodynamic pressure, pad asperities, contact-surface instability and pad-abrasive-workpiece contact. According to Brilliantov and Poschel [33], the total stress $P(x, y, R_b, d, \omega, Y, \nu, \varphi, \eta_1, \eta_2)$ is a sum of the elastic part of the stress tensor σ_{zz}^{el} and the dissipative part of the stress tensor σ_{zz}^{dis} . σ_{zz}^{el} is the known solution for the Hertz contact problem [34] as expressed by Eq. (6) as follows,

$$\sigma_{zz}^{el} = E_1 \frac{\partial u_z}{\partial z} + \left(E_2 - \frac{E_1}{3} \right) \left(\frac{\partial u_x}{\partial x} + \frac{\partial u_y}{\partial y} + \frac{\partial u_z}{\partial z} \right) = p_0 \left(1 - \frac{x^2}{a^2} - \frac{y^2}{a^2} \right)^{1/2} \quad (6)$$

where u_x , u_y and u_z denote the x-, y- and z- direction displacement field of the classic Hertz contact problem; $E_1 = Y / (1 + \nu)$ and $E_2 = Y / 3(1 - 2\nu)$ denote the elastic material constants with Y and ν being the Young modulus and the Poisson ratio of the polishing pad, respectively; $a = \sqrt{dR_b}$ denotes the radius of contact area and $p_0 = 3F_N / (2\pi a^2)$ denotes the maximum contact pressure; F_N is the total elastic force, acting by the surface (in normal direction) on the polishing pad as expressed in Eq. (7):

$$F_N = \frac{2}{3} \frac{Y}{(1 - \nu^2)} R_b^{1/2} d^{3/2} \quad (7)$$

According to the kinematics theory and contact mechanics [33, 35, 36], σ_{zz}^{dis} can be expressed as

$$\sigma_{zz}^{dis} = \eta_1 \frac{\partial \dot{u}_z}{\partial z} + \left(\eta_2 - \frac{\eta_1}{3} \right) \left(\frac{\partial \dot{u}_x}{\partial x} + \frac{\partial \dot{u}_y}{\partial y} + \frac{\partial \dot{u}_z}{\partial z} \right) = \frac{(1 - 2\nu)(1 + \nu)}{Y} \cdot \frac{\omega \cos \varphi (2\eta_2 + \eta_1 / 3) p_0 x (R_b - d)}{a^2} \cdot \left(1 - \frac{x^2}{a^2} - \frac{y^2}{a^2} \right)^{-1/2} + \frac{(1 - \nu)^2}{Y} \cdot \frac{\omega \cos \varphi (2\eta_2 + \eta_1 / 3) \pi p_0 x}{2a} \quad (8)$$

where \dot{u}_x , \dot{u}_y and \dot{u}_z denote the time derivative of the displacement field in x-, y- and z- direction, respectively; η_1 and η_2 are the coefficients of viscosity, related to shear and bulk deformation respectively; ω is the angular velocity; φ is the inclined angle. As a result, the pressure distribution at the polishing contact area can be expressed by

$$P(x, y, R_b, d, \omega, Y, \nu, \varphi, \eta_1, \eta_2) = \sigma_{zz}^{el} + \sigma_{zz}^{dis} = p_0 \left(1 - \frac{x^2}{a^2} - \frac{y^2}{a^2} \right)^{1/2} + \frac{(1-2\nu)(1+\nu)}{Y} \cdot \frac{\omega \cos \varphi (2\eta_2 + \eta_1 / 3) p_0 x (R_b - d)}{a^2} \cdot \left(1 - \frac{x^2}{a^2} - \frac{y^2}{a^2} \right)^{-1/2} + \frac{(1-\nu)^2}{Y} \cdot \frac{\omega \cos \varphi (2\eta_2 + \eta_1 / 3) \pi p_0 x}{2a} \quad (9)$$

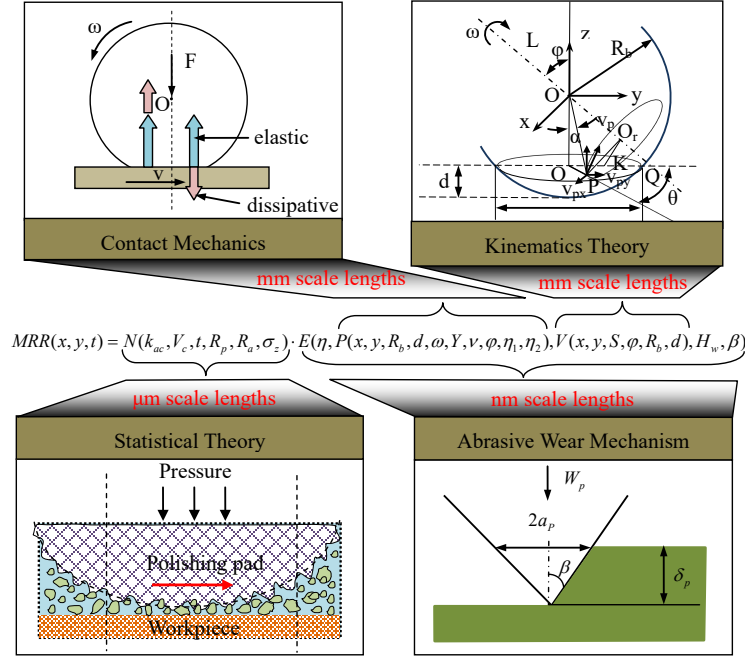


Fig. 4 Schematic illustration of the multi-scale mechanisms affecting the material removal characteristics in bonnet polishing

3.1.2 Surface generation model

In practice, polishing is a multi-step process conducted by repeatedly running particular designed polishing cycles until the expected surface finish and form error are obtained. Within each cycle, the polishing tool sweeps through the **polished** surface under adopted polishing tool path and desired dwell time map. Hence, an important part of the surface generation model is dwell time and tool path planing [37] as considering time efficiency and surface quality improvement. Based on the experimental results of section 2.2.2, bonnet polishing appears to be a relative and cumulative polishing process for various materials and the surface generation, ΔZ_i , of bonnet polishing can be assumed to be a linearly cumulative effect of dwell time, T_0 , together with the material removal rate, MRR_{ij} , under the same polishing condition as follows:

$$\Delta Z_i = \sum_{j=1}^N MRR_{ij} \cdot T_0, \quad (i = 1, 2, 3 \dots M) \quad (10)$$

where M is the sample point number, N is the trajectory point number along the polishing path. and MRR_{ij} is the material removal of j th sample point when the i th trajectory point along the polishing path is polished by the bonnet. The value of MRR_{ij} depends on the material removal rate and the contract area of the bonnet. It will be non-zero if the j th sample point locates within the contract area of the i th trajectory point, and will be zero if the sample point locates outside the contract area.

To verify the predictability of the surface generation model and assess directly the comparison

between measured and predicted results using feature parameters in this study, the polishing conditions in all the paths are assumed to be constant and hence the tool influence function is stable and constant, and the polishing paths are also assumed to be evenly spaced straight lines on a flat surface as can be seen in Fig. 5. When the predicted influence function follows straight path lines with a constant surface feed rate, the removal profile is constant along each and all the path lines. Hence, the material removal distribution is constant along the path line direction and waves in the orthogonal direction arising from the overlapping of the removal profiles affiliated with adjacent polishing path lines for the raster polishing. In this case, the surface generation may be simplified to be a 2D problem which can be solved numerically for given polishing path spacing and path number. The polishing path spacing represents the translation distance of removal profile along the orthogonal direction and the feed rate determines the dwell time of each polished spot and hence the surface height of removal profile along the path line direction.

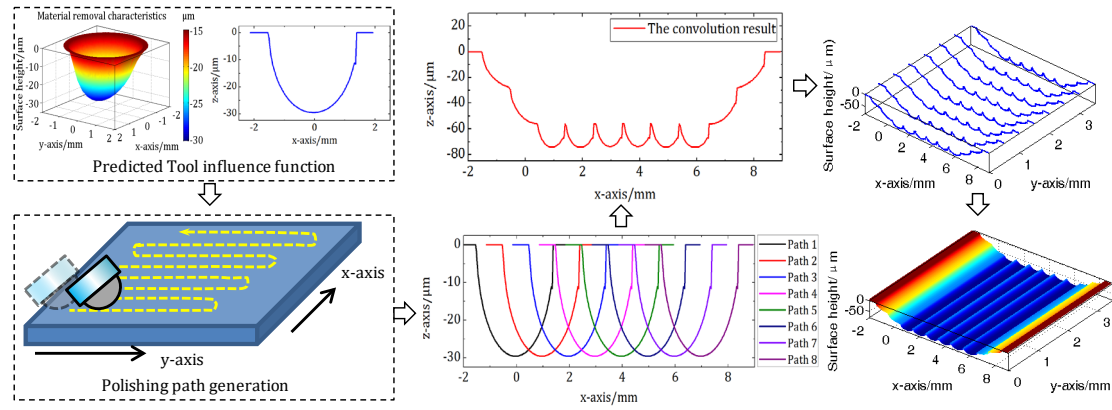


Fig. 5 A schematic diagram of the surface generation model in the raster polishing

3.2 Experimental verification in Part B

In the present study, prototypes of the multi-scale material removal model and the surface generation model for bonnet polishing have been purposely built and programmed by using MATLAB programming software package. Basically, the experimental verification in Part B is divided into two parts, i.e. Part B1 and Part B2. The experiments in Part B1 focus on spot polishing tests which aim to verify the feasibility of the theoretical model under various polishing conditions. The experiment conducted in Part B2 is a pattern test which aims to experimentally evaluate the performance of the surface generation model. A Zeeko IRP 200 ultra-precision freeform polishing machine was used to conduct the experiments. All samples were polished using Al_2O_3 slurry and the surfaces of the samples were measured by a Zygo Nexview 3D Optical Surface Profiler.

3.2.1 Part B1: Experimental verification of the multi-scale material removal model

The multi-scale material removal model for bonnet polishing was verified through a series of simulation and polishing experiments. The predictions of material removal characteristics have been accomplished using the prototype of multi-scale material removal model purposely built by MATLAB

software package. In this study, a bonnet with a radius of 20 mm was assembled on the main spindle, while the workpiece made of steel (S136) was fixed on the C axis. All samples were polished by a LP-66 (Cerium oxide D'27) polishing pad with a slurry comprising 2.066 vol. % of Al_2O_3 abrasives with an average size of 3.22 μm with a constant machining time of 60 seconds. A series of simulations based on the multi-scale material removal model were conducted under various polishing conditions as shown in Table 3, while the coefficients used in the simulations are shown in Table 4.

Table 3 The process parameters of polishing experiments

Sample No.	Tool pressure	Tool offset	Head speed	Precess angle	Slurry concentration
B1	1.2 bar	0.12 mm	1200 rpm	10°	1:12
B2	1.2 bar	0.12 mm	1200 rpm	15°	1:12
B3	1.2 bar	0.12 mm	1200 rpm	20°	1:12
B4	1.2 bar	0.1 mm	900 rpm	15°	1:12
B5	1.2 bar	0.1 mm	1200 rpm	15°	1:12
B6	1.2 bar	0.1 mm	1500 rpm	15°	1:12
B7	1.2 bar	0.08 mm	1200 rpm	15°	1:12
B8	1.2 bar	0.13 mm	1200 rpm	15°	1:12
B9	1.2 bar	0.18mm	1200 rpm	15°	1:12
B10	1.2 bar	0.09 mm	1200 rpm	15°	1:12
B11	1.2 bar	0.09 mm	1200 rpm	15°	1:9
B12	1.2 bar	0.09 mm	1200 rpm	15°	1:6

Table 4 Parameters used in the present simulation

Variable	Symbol	Base value
Young's modulus	Y	2 Mpa
Poisson's ratio	ν	0.3
Viscosity coefficient	η_1	5×10^{-4} Mpa·s
Viscosity coefficient	η_2	0 Mpa·s
Semiangle of cone particle	α	45°
Hardness of workpiece	H_w	509 Mpa
Radius of pad asperities	R_a	23.5 μm
Standard deviation	σ_z	4.4 μm

Fig. 6 shows the predicted and experimental results of the material removal characteristics for case of B1. Fig. 6(a) and 6(b) show the calculated results of velocity and pressure distribution in the polishing area, respectively. Fig. 6(c) shows the experimental data of polished spot measured by Zygo Nexview 3D Optical Surface Profiler, while Fig. 6(d) shows the 3D topography of the material removal characteristics predicted by the multi-scale material removal model. It is found that the predicted result

shows a good agreement with the experimental results. This infers that the contact mechanics and kinematics theory proposed in this study can provide a reasonably well explanation for the polishing mechanisms in bonnet polishing. Moreover, with a consideration of the strong time-dependence of mechanical properties of the polishing bonnet, the model reveals that both of the polishing depth (the down force) and rotational speed have significant effects on the pressure distribution in the polishing area. This helps to explain the asymmetry of the material removal characteristics in X-cross section and Y- cross-section and the phenomenon that the X-Z width of the polished spot was larger than that of the Y-Z width.

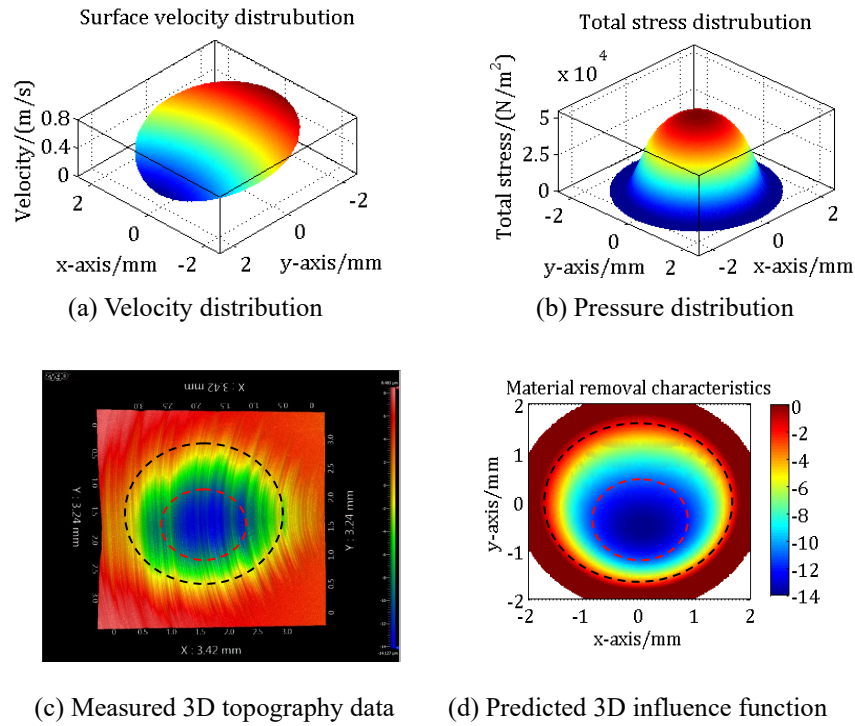


Fig. 6 The simulated and experimental results of the material removal characteristics for case of B1

To further verify the multi-scale material removal model, four sets of simulation and polishing experiments were conducted under various *process* angle, head speed, tool offset and slurry concentration. A comparison between the model predicted and experimental measured results of material removal rate is shown in Fig.7. The multi-scale material removal model is found to predict well for the material removal characteristics under various polishing conditions. As a result, the multi-scale material removal model developed in this study, provides some insights into the contact mechanics and the wear mechanisms underlying the bonnet process.

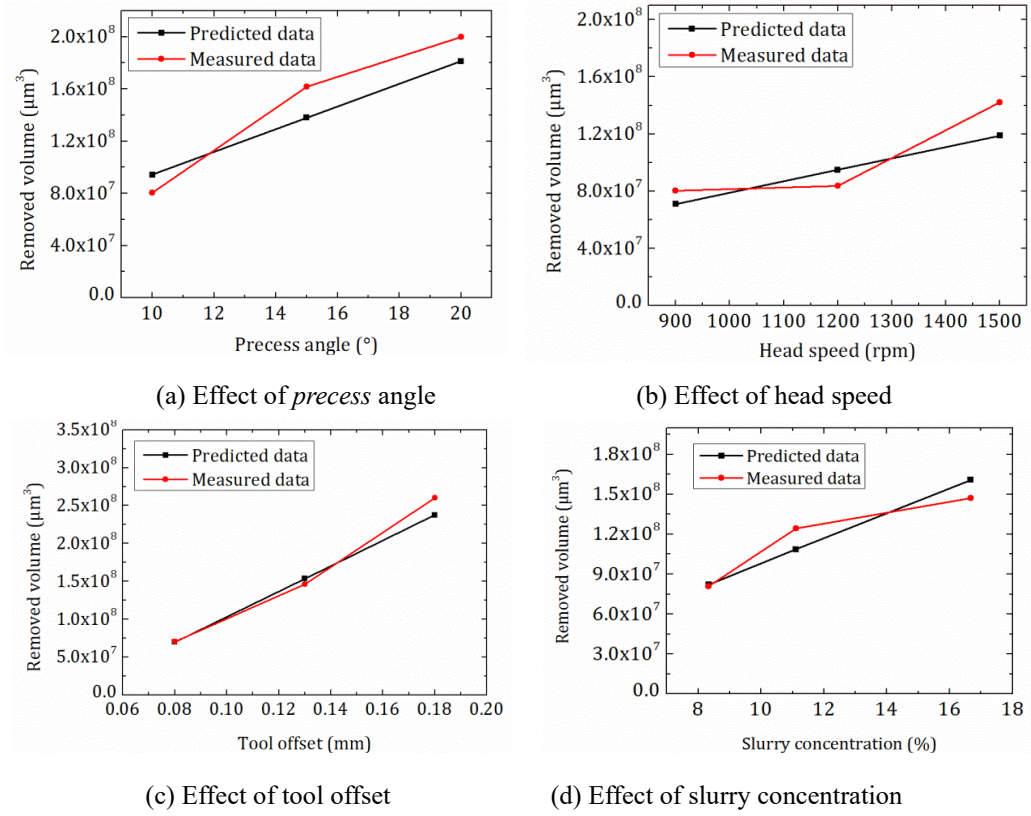


Fig. 7 A comparison of predicted results by the multi-scale material removal model and the experimental results under various polishing conditions

3.2.2 Part B2: Experimental verification of the surface generation model in bonnet polishing

In Part B2, raster polishing experiment has been designed to validate the proposed surface generation model. The polishing strategies used for generating the designed surface pattern are shown in Table 5, while the surface generation model has been purposely built and programmed by using MATLAB software package. Fig. 8 shows a comparison between the measured and simulated results in the pattern test. It is found that the simulated surface pattern by the surface generation model agree well with that for the experimental results. This further validates that the surface generation model can help to explain and predict the relative and cumulative polishing process and the linearly cumulative effect of dwell time together with the constant material removal rate under the identical polishing condition in surface generation of bonnet polishing .

Table 5 Parameters for generating surface pattern

Workpiece Material	Steel (S136)	Polishing mode	Raster
Surface feed	20 mm/min	Polishing cloth	LP-66
Polishing spacing	1 mm	Head speed	1200 rpm
Polishing depth	0.2 mm	<i>Precess</i> angle	15°
Tool pressure	1.2 bar	Slurry concentration	1:12
Tool radius	20 mm	Particle property	3.22 μm (Al_2O_3)

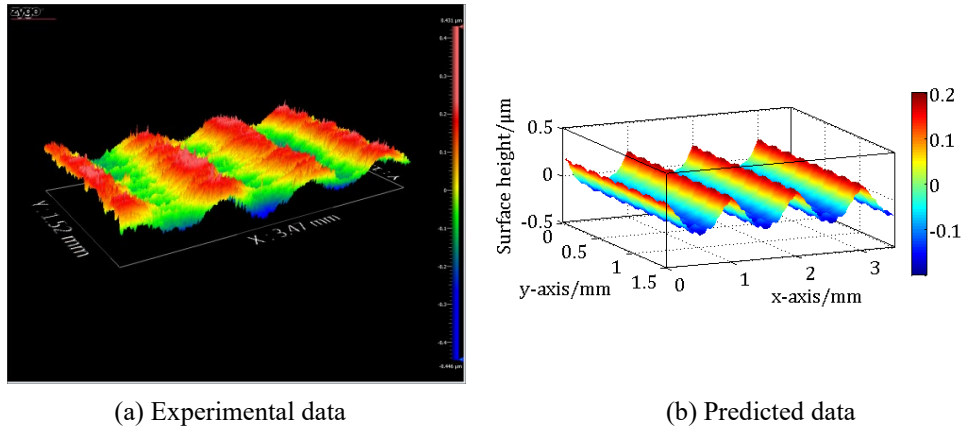


Fig. 8 Comparison between the measured and simulated results of the pattern test

To further verify the effectiveness of the surface generation model, a least-square-based surface matching method is used to evaluate the deviation of the measured surface from the corresponding simulated surface [38]. Due to the misalignment between the coordinate frames of the coordinate frames of the measured surface and the simulated surface, the surface matching is required to search for an optimal Euclidean motion for the measured surface so that it is well aligned with the simulated surface as close as possible. After that, the deviation of the simulated surface and the measured surface is considered to be the prediction error of the proposed model as shown in Fig. 9. It is turned out that the peak-to-valley value (PV) of the prediction error is $0.4231\ \mu\text{m}$ and the root-mean-squared value (RMS) is $64.8\ \text{nm}$. The result reveals that the surface generation model can be successfully used for predicting and better explaining the surface generation in bonnet polishing. This further validates the technical feasibility and effectiveness of the surface generation model in bonnet polishing.

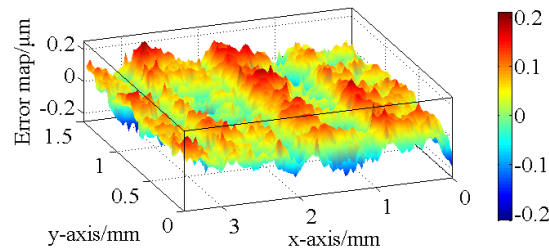


Fig. 9 Evaluated prediction error of the testing pattern for bonnet polishing

4. Conclusions

This paper presents a theoretical and experimental investigation which attempts to gain a better scientific understanding of the material removal characteristics and surface generation mechanisms in bonnet polishing. The major findings are summarized as follows:

- (i) Material removal and surface generation mechanisms were studied through a series of polishing experiments. Although the material removal is shared by the abrasive particles and the pad asperities in the designed experiments, the abrasive wear occurred in bonnet polishing is dominated significantly by

plastic removal mode of abrasive particles, while the material removal caused by the polishing pad should be mitigated in order to obtain super mirror finished surfaces without pad scratches. Experimental results also reveal that the surface generation of bonnet polishing is a linearly cumulative effect of dwell time together with the constant material removal rate for the identical polishing condition.

(ii) Hence, a multi-scale material removal model is built for predicting and characterizing the materials removal characteristics in bonnet polishing based on the study of contact mechanics, kinematics theory and abrasive wear mechanism. It reveals that both of the polishing depth (the down force) and rotational speed have significant effects on the pressure distribution in the polishing area, and hence this can explain the asymmetry of the material removal characteristics in X-cross-section and Y-cross-section. It is also found that the X-Z width of the polished spot is larger than the Y-Z width. A surface generation model is also built to take account of the relative and cumulative removal process together with the predicted material removal characteristics.

(iii) A series of spot and pattern polishing tests as well as simulation experiments were conducted. The results show that the theoretical model predicts well for the amount of material removal which not only increases with increasing *precess* angle and tool offset, but also depends linearly on the head speed and slurry concentration. Through the experimental study and theoretical analysis by the surface generation model, it is also found that a relative and cumulative process is proven to be a key surface generation mechanism in bonnet polishing.

Acknowledgement

The work described in this paper was fully supported by a grant from the Research Grants Council of the Government of the Hong Kong Special Administrative Region, China (Project No.: PolyU 5132/11E). The work was also supported by a PhD studentship (project code: RTC3) from The Hong Kong Polytechnic University.

Reference

- [1] D.D. Walker, R. Freeman, G. McCavana, R. Morton, D. Riley, J. Simms, D. Brooks, E.D. Kim, A. King, The Zeeko/UCL process for polishing large lenses and prisms, *Large Lenses and Prism*, 4411 (2002) 106-111.
- [2] A. Beaucamp, Y. Namba, Super-smooth finishing of diamond turned hard X-ray molding dies by combined fluid jet and bonnet polishing, *CIRP Annals - Manufacturing Technology*, 62 (2013) 315-318.
- [3] P. Charlton, L. Blunt, Surface and form metrology of polished “freeform” biological surfaces, *Wear*, 264 (2008) 394-399.
- [4] C.F. Cheung, L.T. Ho, P. Charlton, L.B. Kong, S. To, W.B. Lee, Analysis of surface generation in the ultraprecision polishing of freeform surfaces, *Proceedings of the Institution of Mechanical Engineers, Part B: Journal of Engineering Manufacture*, 224 (2010) 59-73.

- [5] A. Beaucamp, Y. Namba, P. Charlton, Corrective finishing of extreme ultraviolet photomask blanks by precessed bonnet polisher, *Appl Optics*, 53 (2014) 3075-3080.
- [6] D.D. Walker, D. Brooks, R. Freeman, A. King, G. McCavana, R. Morton, D. Riley, J. Simms, The first aspheric form and texture results from a production machine embodying the Precession Process, *Optical Manufacturing and Testing Iv*, 4451 (2001) 267-276.
- [7] D. Walker, G.Y. Yu, H.Y. Li, W. Messelink, R. Evans, A. Beaucamp, Edges in CNC polishing: from mirror-segments towards semiconductors, paper 1: edges on processing the global surface, *Opt Express*, 20 (2012) 19787-19798.
- [8] Y. Kakinuma, K. Igarashi, S. Katsura, T. Aoyama, Development of 5-axis polishing machine capable of simultaneous trajectory, posture, and force control, *CIRP Annals - Manufacturing Technology*, 62 (2013) 379-382.
- [9] M.J. Tsai, J.F. Huang, W.L. Kao, Robotic polishing of precision molds with uniform material removal control, *International Journal of Machine Tools and Manufacture*, 49 (2009) 885-895.
- [10] C.J. Evans, E. Paul, D. Dornfeld, D.A. Lucca, G. Byrne, M. Tricard, F. Klocke, O. Dambon, B.A. Mullany, Material Removal Mechanisms in Lapping and Polishing, *CIRP Annals - Manufacturing Technology*, 52 (2003) 611-633.
- [11] Y.S. Xie, B. Bhushan, Effects of particle size, polishing pad and contact pressure in free abrasive polishing, *Wear*, 200 (1996) 281-295.
- [12] J. Seok, C.P. Sukam, A.T. Kim, J.A. Tichy, T.S. Cale, Material removal model for chemical-mechanical polishing considering wafer flexibility and edge effects, *Wear*, 257 (2004) 496-508.
- [13] S.J. Eder, U. Cihak-Bayr, A. Pauschitz, Nanotribological simulations of multi-grit polishing and grinding, *Wear*.
- [14] H. Xu, K. Komvopoulos, A Quasi-Static Mechanics Analysis of Three-Dimensional Nanoscale Surface Polishing, *J Manuf Sci E-T Asme*, 132 (2010).
- [15] Z.C. Cao, C.F. Cheung, Theoretical modelling and analysis of the material removal characteristics in fluid jet polishing, *Int J Mech Sci*, 89 (2014) 158-166.
- [16] J. Tichy, J.A. Levert, L. Shan, S. Danyluk, Contact mechanics and lubrication hydrodynamics of chemical mechanical polishing, *J Electrochem Soc*, 146 (1999) 1523-1528.
- [17] A. Beaucamp, Y. Namba, I. Inasaki, H. Combrinck, R. Freeman, Finishing of optical moulds to $\lambda/20$ by automated corrective polishing, *CIRP Annals - Manufacturing Technology*, 60 (2011) 375-378.
- [18] C.F. Cheung, L.B. Kong, L.T. Ho, S. To, Modelling and simulation of structure surface generation using computer controlled ultra-precision polishing, *Precis Eng*, 35 (2011) 574-590.
- [19] S.Y. Zeng, L. Blunt, Experimental investigation and analytical modelling of the effects of process parameters on material removal rate for bonnet polishing of cobalt chrome alloy, *Precis Eng*, 38 (2014) 348-355.
- [20] M. Schinhaerl, R. Rascher, R. Stamp, G. Smith, L. Smith, E. Pitschke, P. Sperber, Filter algorithm for influence functions in the computer controlled polishing of high-quality optical lenses, *International*

Journal of Machine Tools and Manufacture, 47 (2007) 107-111.

[21] N. Saka, T. Eusner, J.H. Chun, Scratching by pad asperities in chemical–mechanical polishing, CIRP Annals - Manufacturing Technology, 59 (2010) 329-332.

[22] I.M. Hutchings, Mechanisms of Wear in Powder Technology - a Review, Powder Technol, 76 (1993) 3-13.

[23] S. Kim, N. Saka, J.H. Chun, S.H. Shin, Modeling and mitigation of pad scratching in chemical–mechanical polishing, CIRP Annals - Manufacturing Technology, 62 (2013) 307-310.

[24] S. Kim, N. Saka, J.-H. Chun, The Effect of Pad-asperity Curvature on Material Removal Rate in Chemical-mechanical Polishing, Procedia CIRP, 14 (2014) 42-47.

[25] J. Greenwood, J. Williamson, Contact of nominally flat surfaces, Proceedings of the Royal Society of London. Series A. Mathematical and Physical Sciences, 295 (1966) 300-319.

[26] G.H. Fu, A. Chandra, S. Guha, G. Subhash, A plasticity-based model of material removal in chemical-mechanical polishing (CMP), Ieee T Semiconduct M, 14 (2001) 406-417.

[27] J.F. Luo, D.A. Dornfeld, Effects of abrasive size distribution in chemical mechanical planarization: Modeling and verification, Ieee T Semiconduct M, 16 (2003) 469-476.

[28] J.F. Luo, D.A. Dornfeld, Material removal mechanism in chemical mechanical polishing: Theory and modeling, Ieee T Semiconduct M, 14 (2001) 112-133.

[29] J.M. Challen, P.L.B. Oxley, An explanation of the different regimes of friction and wear using asperity deformation models, Wear, 53 (1979) 229-243.

[30] I.M. Hutchings, Tribology: friction and wear of engineering materials, (1992).

[31] K. Hokkirigawa, K. Kato, An experimental and theoretical investigation of ploughing, cutting and wedge formation during abrasive wear, Tribol Int, 21 (1988) 51-57.

[32] M.S. Bingley, S. Schnee, A study of the mechanisms of abrasive wear for ductile metals under wet and dry three-body conditions, Wear, 258 (2005) 50-61.

[33] N.V. Brilliantov, T. Poschel, Rolling friction of a viscous sphere on a hard plane, Europhys Lett, 42 (1998) 511-516.

[34] L.D. Landau, E.M. Lifshitz, Theory of Elasticity, Pergamon Press, 1959.

[35] Q.J. Zheng, H.P. Zhu, A.B. Yu, Finite element analysis of the rolling friction of a viscous particle on a rigid plane, Powder Technol, 207 (2011) 401-406.

[36] K.L. Johnson, K.L. Johnson, Contact mechanics, Cambridge university press, 1987.

[37] H.Y. Tam, O.C.H. Lui, A.C.K. Mok, Robotic polishing of free-form surfaces using scanning paths, J Mater Process Tech, 95 (1999) 191-200.

[38] M.J. Ren, C.F. Cheung, L.B. Kong, A task specific uncertainty analysis method for least-squares-based form characterization of ultra-precision freeform surfaces, Meas Sci Technol, 23 (2012).

List of Figure Caption

- Fig.1 (a) Configure and (b) schematic illustration of bonnet polishing
- Fig.2 (a) Zeeko IRP200 Ultra-precision freeform polishing machine, (b) Zygo Nexview 3D Optical Surface Profiler and (c) HITACHI TM3000 Tabletop Scanning Electron Microscope
- Fig.3 The effect of polishing time on the surface generation
- Fig.4 Schematic illustration of the multi-scale mechanisms affecting the material removal characteristics in bonnet polishing
- Fig.5 A schematic diagram of the surface generation model in the raster polishing
- Fig.6 The simulated and experimental results of the material removal characteristics for case of B1
- Fig.7 A comparison of predicted results by the multi-scale material removal model and the experimental results under various polishing conditions
- Fig.8 Comparison between the measured and simulated results of the pattern test
- Fig.9 Evaluated prediction error of the testing pattern for bonnet polishing